

Wave Concept Iterative Method for Waveguide Filter Modeling

^{1*} Mr.Pradosh Ranjan Parida, ² Mr.Ajit ku Mohapatra
^{1*} *Asst. Professor, Dept. Of Electrical Engineering, NIT BBSR,*
Asst. Professor DEPT. of Electrical Engineering, NIT BBSR,
pradoshranjan@thenalanda.com, ajit@thenalanda.com

Abstract

A challenging frequency selective surface is designed using a strict full wave method based on the Transverse Wave Concept Iterative Process (WCIP) (FSS). These surfaces have a regularly occurring array of identical circuits. In deep space operations for multiple frequencies, they are used as filters and reflector antennas. The first stage of our method's validation involves studying a straightforward FSS structure. Two different complex structures are explored in the second stage. The design process is warranted by the high degree of agreement between simulations and published data..

Keywords

FSS, WCIP, Wave, 2D-FFT Algorithm

1. Introduction

Frequency Selective Surfaces (FSS), which find widespread applications as filters for microwaves and optical signals, have been the subject of extensive studies in recent years [1] [2] [3] [4]. These surfaces include periodically arranged metallic patch elements or aperture elements within a metallic screen and exhibit total reflection (patches) or Transmission (apertures) in the neighborhood of the element resonance [1]. Their performances depend on the substrate characteristics, element type, dimensions and the spacing between elements.

The response parameters are predicted by analyzing the surface using different techniques [5] [6] [7]. However, the small dimensions of the circuit producesome problems in result precisions. Thus, the coupling conditions between the different elements must be taken into account. Then, the efficiency of the used method, their memory consumption and time requirement are usually made these methods unsuitable for optimization.

This paper presents the analysis of simple and complex passive FSS by the iterative method (WCIP). The WCIP technique takes the advantage of simplicity in its procedure based on Fast Modal Transform (FMT) in the passage between spatial and spectral domain [8] [9]. In addition, there is no matrix inversion was required and the convergence was insured independently of the circuit complexity. Further, there is unlimited shapes of circuit are imposed [10]. The simulation results are validated with those calculated with HFSS commercial code and recently published experimental results.

2. Theory: WCIP Formulation

The general Frequency Selective Surface structure is depicted in **Figure 1**. The circuit interface is constituted of two sub domains: metal and dielectric. It is de-posed on homogeneous dielectric substrate with thickness h and permittivity ϵ_r .

WCIP method is based on the full wave transverse wave formulation and the on collection of information at the interfaces. A multiple reflection procedure is started using initial conditions and stopped once convergence which is achieved. Two related operators incidented waves and scattered waves in the spatial do- main and in the spectral domain governs the iterative procedure. They are: the scattng operator S_{Ω} and the reflection R_{Ω} .

As shown in **Figure 2**, the incident waves A_i and the scattered waves B_j are calculated from the tangential electric and magnetic fields

E_i and H_i

as:

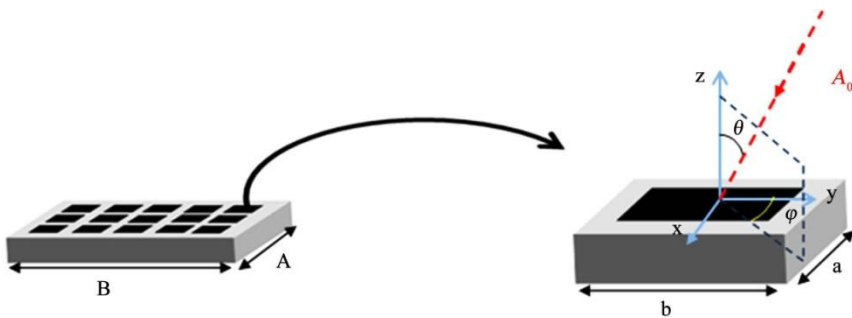


Figure 1. Periodic structure (FSS) with unit cell.

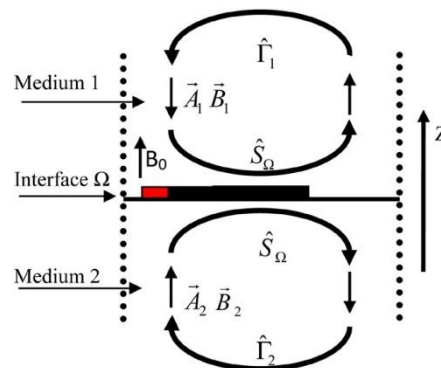


Figure 2. Iterative process.

$$\begin{aligned}
 & \vec{E}_i = \vec{E}_0 + \sum_{i=1}^{\infty} \vec{E}_i \\
 & \vec{H}_i = \vec{H}_0 + \sum_{i=1}^{\infty} \vec{H}_i \\
 & \vec{B}_i = \vec{B}_0 + \sum_{i=1}^{\infty} \vec{B}_i \\
 & \vec{A}_i = \vec{A}_0 + \sum_{i=1}^{\infty} \vec{A}_i \\
 & \vec{J}_i = \vec{J}_0 + \sum_{i=1}^{\infty} \vec{J}_i \\
 & \vec{Z}_i = \vec{Z}_0 + \sum_{i=1}^{\infty} \vec{Z}_i
 \end{aligned}$$

$$\sqrt{Z_{0i}}$$

where i indicates the medium 1 or 2 corresponding to a given interface Ω .

Z_{0i}

is the characteristic impedance of the same medium i and \mathbf{J}_i

current density vector given as: being the surface

$$\mathbf{J}_i = \mathbf{H}_i \times \mathbf{n} \quad (2)$$

with \mathbf{n} being the outward vector normal to the interface. Thus, the tangential electric and magnetic fields can be calculated from:

$$\sqrt{Z_{0i}} \mathbf{E}_i = \mathbf{A}_i - \mathbf{B}_i$$

$$\sqrt{Z_{0i}} \mathbf{J}_i = \mathbf{A}_i + \mathbf{B}_i$$

$$\sqrt{Z_{0i}} \mathbf{J}_i = \mathbf{A}_i + \mathbf{B}_i$$

$$\sqrt{Z_{0i}} \mathbf{J}_i = \mathbf{A}_i + \mathbf{B}_i \quad (3.1)$$

$$(3.2)$$

The scattered waves are related to the incident waves as:

$$\mathbf{B}_2 = S \mathbf{A}_1$$

$$\mathbf{B}_1 = S \mathbf{A}_2$$

$$\mathbf{B}_1 = S \mathbf{A}_1 \quad (4)$$

S is a scattering operator defines in the spatial and it accounts for the boundary conditions. The scattered waves \mathbf{B}_i will be reflect to generate the incident waves for the next iteration but after adding the incident source waves \mathbf{A}_0 :

\mathbf{A}_0 :

$$\mathbf{A}_2 = \mathbf{A}_0 + \mathbf{B}_1$$

$$\mathbf{A}_1 = \mathbf{A}_0 + \mathbf{B}_2 \quad (5)$$

\mathbf{R}_i being the reflection operator and it is defined in the spectral domain.

Scattering Operator Determination

Two domains characterizing the interface Ω of a loaded FSS are: the dielectric domain and the metal domain. They can be represented using Heaviside unit steps as:

$$D = \begin{cases} 1 & \text{on the dielectric} \\ 0 & \text{otherwise} \end{cases} \quad H = \begin{cases} 1 & \text{on the dielectric} \\ 0 & \text{otherwise} \end{cases}$$

$$M = \begin{cases} 1 & \text{on the metal} \\ 0 & \text{otherwise} \end{cases} \quad H = \begin{cases} 1 & \text{on the metal} \\ 0 & \text{otherwise} \end{cases} \quad (6.1)$$

$$(6.2)$$

The boundary conditions on the metal domain H_M are:

$$E_1 = E_2 = 0 \quad (7)$$

Replacing (3) in (7) results in:

$$\sqrt{Z_{01}} A_1 = \sqrt{Z_{02}} B_1 \quad (8)$$

The metal domain scattering operator

$$\sqrt{Z_{02}} A_2 = \sqrt{Z_{01}} B_2 = 0 \quad (8)$$

lic domain generator H_M

y:

S_M is given in the terms of the metal-

S

$$S_M = H_M \quad (9)$$

$$S_M = H_M \quad (9)$$

In the dielectric domain, the boundary conditions which be satisfied on the interface are:

$$J_{tot} = J_1 = J_2 = 0 \quad (10)$$

$$E_1 = E_2$$

1

2

Using (3) and (10), and defining N domain

$\sqrt{Z_{01}/Z_{02}}$, thus, the dielectric

scattering operator

S_D can be given terms of the dielectric generator H_D

as:

$$S_D = \frac{1}{N^2} H_D$$

$$S_D = \frac{2}{1 + N^2} H_D$$

$$S_D = \frac{1}{1 + N^2} H_D$$

$$S_D = \frac{2}{1 + N^2} H_D \quad (11)$$

In the lumped elements domain, the boundary to be verified is given by:

$$E_1 \square E_2 \square Z_s \square J_1 \square J_2 \square$$

Then, the total scattering operator $S \square$ is given as:

$$S \square \square S_M \square S_D$$

(12)

(13)

Reflection Operator Determination

The modes are decoupled in the domain of modes where each mode is characterized by its own reflection coefficient, the need to pass to spectral domain is necessary. To enable this operation, a transform known as the Fast Modal Transform FMT defined and to go back to spatial domain, FMT^{-1} is will be used.

The reflection coefficient in the spectral domain is given by:

$$\Gamma_{imn} = \frac{1 - Z_{imn} Y_{imn}}{1 + Z_{imn} Y_{imn}}$$

(14)

where Y_{imn} is the admittance of the mn mode at the medium i and Γ_{imn} stands

for the modes TE or TM. When no closing ends exist,

Y_{imn} can be calculated by [5] [6]:

$$Y_{imn}^{TM} = \frac{j\omega \epsilon_0 \epsilon_{ri}}{y_{imn}}$$

(15)

$$Y_{imn}^{TE} = \frac{y_{mn}}{j\omega \mu_0 \mu_{ri}}$$

(16)

0

being the propagation constant of the medium i and it is given by (19).

ϵ_0 ,

ϵ_{ri}

and

ϵ_0 are permittivity of the vacuum, the relative of the medium i and the permeability of the vacuum respectively.

Due to the closed packaging, two types of modes are coupled; the modes of the small guide and those of the global guide.

The global guide is classical a rectangular wave guide with electric walls. The bases functions are sinus and cosinus.

Then there are described extensively in [9] and [10]. The small guide is a 2D periodic guide, and the bases functions are exponential. There are described in [8].

As consequence, the global general function becomes:

$$\begin{aligned}
 & \frac{1}{\sqrt{ab}} \left[\sum_{m=0}^{\infty} \sum_{n=0}^{\infty} \frac{e^{-\gamma_{mn} z}}{\gamma_{mn}} \cos\left(\frac{2m\pi}{a} x\right) \cos\left(\frac{2n\pi}{b} y\right) \right] \\
 & + \frac{1}{\sqrt{ab}} \left[\sum_{m=0}^{\infty} \sum_{n=0}^{\infty} \frac{e^{-\gamma_{mn} z}}{\gamma_{mn}} \sin\left(\frac{2m\pi}{a} x\right) \sin\left(\frac{2n\pi}{b} y\right) \right] \\
 & + \frac{1}{\sqrt{ab}} \left[\sum_{m=0}^{\infty} \sum_{n=0}^{\infty} \frac{e^{-\gamma_{mn} z}}{\gamma_{mn}} \cos\left(\frac{2m\pi}{a} x\right) \sin\left(\frac{2n\pi}{b} y\right) \right] \\
 & + \frac{1}{\sqrt{ab}} \left[\sum_{m=0}^{\infty} \sum_{n=0}^{\infty} \frac{e^{-\gamma_{mn} z}}{\gamma_{mn}} \sin\left(\frac{2m\pi}{a} x\right) \cos\left(\frac{2n\pi}{b} y\right) \right] \\
 & \left[A e^{-\gamma_{mn} z} + B e^{\gamma_{mn} z} \right] \cos\left(\frac{2m\pi}{a} x\right) \cos\left(\frac{2n\pi}{b} y\right) \\
 & \left[A e^{-\gamma_{mn} z} + B e^{\gamma_{mn} z} \right] \sin\left(\frac{2m\pi}{a} x\right) \sin\left(\frac{2n\pi}{b} y\right) \\
 & \left[A e^{-\gamma_{mn} z} + B e^{\gamma_{mn} z} \right] \cos\left(\frac{2m\pi}{a} x\right) \sin\left(\frac{2n\pi}{b} y\right) \\
 & \left[A e^{-\gamma_{mn} z} + B e^{\gamma_{mn} z} \right] \sin\left(\frac{2m\pi}{a} x\right) \cos\left(\frac{2n\pi}{b} y\right)
 \end{aligned}$$

$$\begin{aligned}
 & \frac{1}{\sqrt{ab}} \left[\sum_{m=0}^{\infty} \sum_{n=0}^{\infty} \frac{e^{-\gamma_{mn} z}}{\gamma_{mn}} \cos\left(\frac{2m\pi}{a} x\right) \cos\left(\frac{2n\pi}{b} y\right) \right] \\
 & + \frac{1}{\sqrt{ab}} \left[\sum_{m=0}^{\infty} \sum_{n=0}^{\infty} \frac{e^{-\gamma_{mn} z}}{\gamma_{mn}} \sin\left(\frac{2m\pi}{a} x\right) \sin\left(\frac{2n\pi}{b} y\right) \right] \\
 & + \frac{1}{\sqrt{ab}} \left[\sum_{m=0}^{\infty} \sum_{n=0}^{\infty} \frac{e^{-\gamma_{mn} z}}{\gamma_{mn}} \cos\left(\frac{2m\pi}{a} x\right) \sin\left(\frac{2n\pi}{b} y\right) \right] \\
 & + \frac{1}{\sqrt{ab}} \left[\sum_{m=0}^{\infty} \sum_{n=0}^{\infty} \frac{e^{-\gamma_{mn} z}}{\gamma_{mn}} \sin\left(\frac{2m\pi}{a} x\right) \cos\left(\frac{2n\pi}{b} y\right) \right] \\
 & \left[A e^{-\gamma_{mn} z} + B e^{\gamma_{mn} z} \right] \cos\left(\frac{2m\pi}{a} x\right) \cos\left(\frac{2n\pi}{b} y\right) \\
 & \left[A e^{-\gamma_{mn} z} + B e^{\gamma_{mn} z} \right] \sin\left(\frac{2m\pi}{a} x\right) \sin\left(\frac{2n\pi}{b} y\right) \\
 & \left[A e^{-\gamma_{mn} z} + B e^{\gamma_{mn} z} \right] \cos\left(\frac{2m\pi}{a} x\right) \sin\left(\frac{2n\pi}{b} y\right) \\
 & \left[A e^{-\gamma_{mn} z} + B e^{\gamma_{mn} z} \right] \sin\left(\frac{2m\pi}{a} x\right) \cos\left(\frac{2n\pi}{b} y\right)
 \end{aligned}$$

A

$$\begin{aligned}
 & \frac{2m\pi}{a} \quad \frac{2p\pi}{b} \\
 & \frac{j\frac{2m\pi}{a} + \frac{2p\pi}{b}}{\sqrt{ab} \sqrt{\left(\frac{2m\pi}{a} + \frac{2p\pi}{b}\right)^2 + \left(\frac{2n\pi}{B} + \frac{2q\pi}{b}\right)^2}} e^{-j\frac{2m\pi}{a}x} e^{-j\frac{2n\pi}{B}y} \\
 & \frac{A}{B} e^{-j\frac{2m\pi}{a}x} e^{-j\frac{2n\pi}{B}y}
 \end{aligned}$$

B

$$\begin{aligned}
 & \frac{2n\pi}{B} \quad \frac{2q\pi}{b} \\
 (18) \\
 & \frac{j\frac{2p\pi}{a} + \frac{2n\pi}{B}}{\sqrt{ab} \sqrt{\left(\frac{2m\pi}{a} + \frac{2p\pi}{b}\right)^2 + \left(\frac{2n\pi}{B} + \frac{2q\pi}{b}\right)^2}} e^{-j\frac{2m\pi}{a}x} e^{-j\frac{2n\pi}{B}y} \\
 & \frac{A}{B} e^{-j\frac{2m\pi}{a}x} e^{-j\frac{2n\pi}{B}y}
 \end{aligned}$$

and the constant of propagation becomes:

$$\gamma_{mn} = \sqrt{\left(\frac{2m\pi}{a} + \frac{2p\pi}{b}\right)^2 + \left(\frac{2n\pi}{B} + \frac{2q\pi}{b}\right)^2 - K_0^2 \epsilon_{ri}} \quad (19)$$

The terms: $\frac{2m\pi}{a}$ and $\frac{2p\pi}{b}$ and $\frac{2n\pi}{B}$ and $\frac{2q\pi}{b}$ described the small and global guides modes coupling, p, q, m and $n = 1, 2, 3, 4, \dots$.

Fast Modal Transform FMT

The FMT/FMT⁻¹ pair permits to go from spatial domain to the spectral domain and back to the spatial domain [7]. It is summarized in the following two equations.

The use of the FMT requires that the space and spectral fields are discrete. In the space fields this discretization is carried out by a grid in small rectangular areas (pixels) of the interface Ω . Electromagnetic value and the incidental and reected waves are represented by matrices whose dimensions depend on the density of grid of this interface. The FMT makes it possible to define the amplitudes of the modes TE and TM in the spectral fields.

$$\begin{aligned}
 & \dots \\
 & E_x(x, y) \\
 & \dots
 \end{aligned}$$

$$B_{TE}^{TE}$$

$$N_{ymn}$$

$$N_{xmn}$$

$$E_x(x, y)$$

FMT

$$E_y(x, y)$$

$$mn$$

$$TM \quad N_{xmn}$$

$$B_{mn}$$

$$N_{ymn}$$

$$fft2$$

$$E_y(x, y)$$

(20)

$$E_x(x, y)$$

$$N_{ymn}$$

$$N_{xmn}$$

$$B^{TE}$$

B^{TE}

$$mn \quad TM$$

$$mn$$

B

$$E_y(x, y)$$

$$fft2^{-1}$$

$$N_{xmn}$$

$$N_{ymn}$$

$$mn \quad TM$$

$$mn$$

(21)

B

$$\frac{m}{a} \quad mn$$

1

$-N$

$$\sqrt{\frac{m^2}{a^2} + \frac{n^2}{b^2}}$$

N_{xmn}

where

and
 N_{mn}

N_{ymn}

mn

$\frac{1}{b}$

N

3. Study of the Numerical Complexity and the Convergence of the Method

To compare the numerical complexity of these two methods, we consider Q like the total number of pixels in the field of the interface and Q_m is the number of pixel in the metal field. Q_m corresponds to the number of useful Roof tops (roof useful signals) for the method of moment. The total number of operation is given by the Equations (1.33) (1.34), [11].

Iterative method W.C.I.P. (K iteration)

$$\text{Oper}_{\text{WCIP}} = 4kQ + 1 + 3\log_2 Q$$

Method of moments

$$R = Q Q_m$$

$$\text{Oper}_{\text{MoM}} = 3R^3$$

Figure 3 shows the evolution of a number of operations according to the percentage of metallization. The point of intersections between the two curves (point “M”) corresponds to 20% of metallization and 0.0121×10^{10} operations. It is calculated with a grid of 64×64 cells and 200 iterations.

The latter is based on the method of the moments. This method is very interesting since it is employed by the majority of the most important editors of electromagnetic simulators [9]. An evaluation of the number of fundamental operations in the iterative method (F.W.C.I.P) and the method of moments showed that starting from a certain density of grid of the study structure (**Figure 3**), the economy in a number of operations, therefore in computing times, is then considerable and widely justifies the use of the F.W.C.I.P. compared to the method of the moments. Moreover the iterative method is always convergent and the absence of the functions of test facilitates its implementation, which allows a fast and total design of microwaves circuits to be realized.

4. Application and Experimental Results

A practical application has been developed starting from the above considerations, so designing a waveguide filter to be inserted in a very small aperture

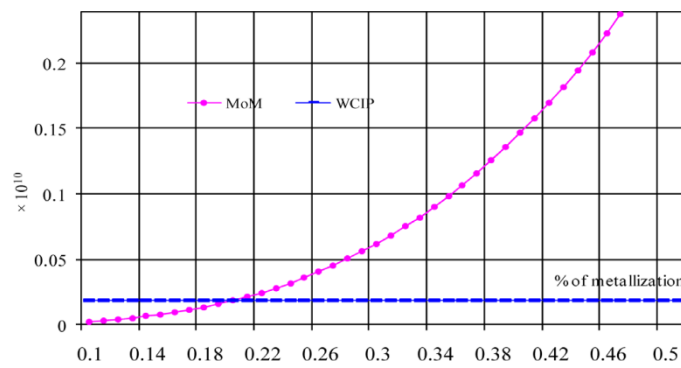
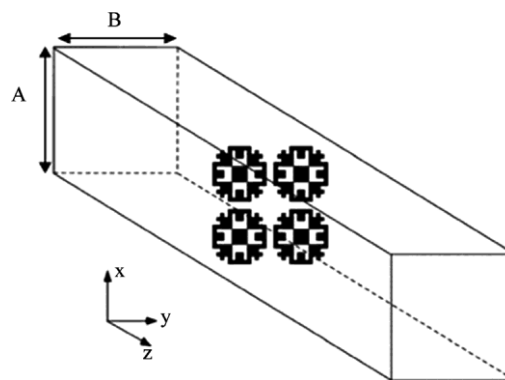
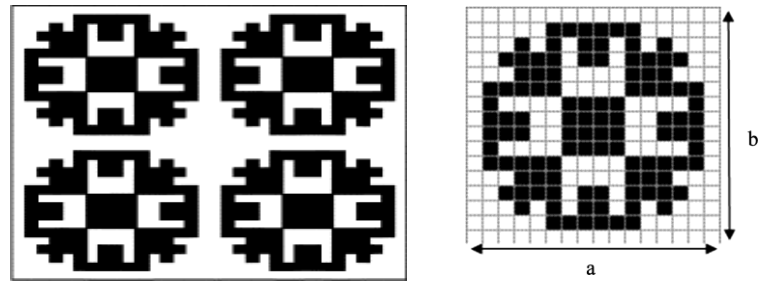


Figure 3. Evolution of necessary calculated time for the two methods W.C.I.P and MoM.

terminal (VSAT) feeder. The terminal has to operate in a dual-band and dual-polarization mode, both transmitting toward and receiving data from a satellite operating at two frequency bands. Traditional solutions consist in using a two-feeder single-focus system, or a dichroic sub-reflector or a shaped reflector double-focus system. The first solution is clearly the most inexpensive but it is liable to astigmatism problems, since it employs a common focus for two feeders. Dichroic surfaces are widely used in radio astronomy, but they require an accurate assembly and are not so compact and low cost as such mass production requires. Finally, shaped reflectors need a precise and expensive construction. To obtain a simple, robust, and low-cost project, we adopted a single feeder with a single focus system; in particular, the feeder has been designed on the basis of a three-port diplexer which separates the K and the Ku signals. An FSS has been inserted inside the waveguide; it results to be transparent at the higher frequency bands, K and Ku, but reflecting the lower band. The reflected waves are therefore forced to enter into the port where both good matching and low insertion loss are required over a very wide frequency band (10.7 - 12.75 GHz). Moreover, the reflection section realized by the FSS can be properly positioned in order to reduce the spurious coupling of the higher frequency signals into the X/Ku port and then to simplify the relevant rejection filter. Finally, the FSS section allows us to design the K and Ku sections as a typical dual band ortho mode transducer (OMT). As shown in **Figure 4**, The FSS consists of a thin Kapton sheet, on



(a)



(b)

(c)

Figure 4. Filter within the waveguide; axis z denotes the propagation direction along the waveguide (a). Basic unit cell (b) derived by the GA and a complete view of the resulting FSS filter (c) $a = b = 0.916$.

which specific metallic elements are printed. The permittivity of the dielectric substrate is, and its thickness is 25 mm, it follows that the incidence angle θ may vary in the range 40.03° in the band, and in the ranges 22.8° and 16.4° in the two pass-bands, respectively. WR90 waveguide ($A = 22.86$ mm, $B = 10.16$ mm, $a = b = 0.916$ cm) excitation the iterative process is stopped after 200 iteration (**Figure 5**). Structures studied in this paper are generated by genetic algorithms, to identify the dimension are reference mesh.

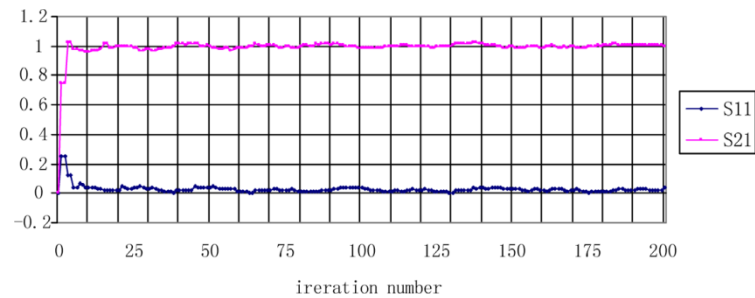


Figure 5. Convergence of S_{11} and S_{21} according to the number of iteration.

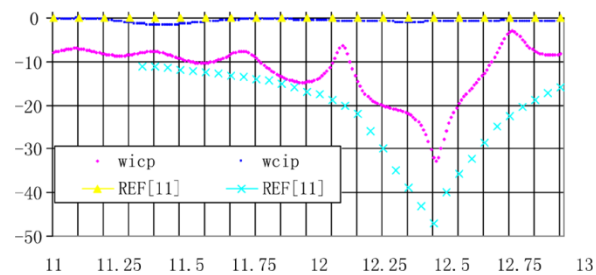


Figure 6. Variation of transmission and reflection coefficients as a function of frequency ($\theta = 40.03^\circ$).

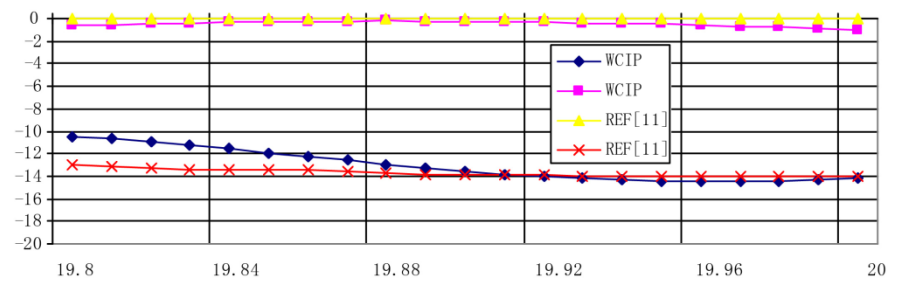


Figure 7. Variation of transmission and reflection coefficients as a function of frequency ($\theta = 22.8^\circ$).

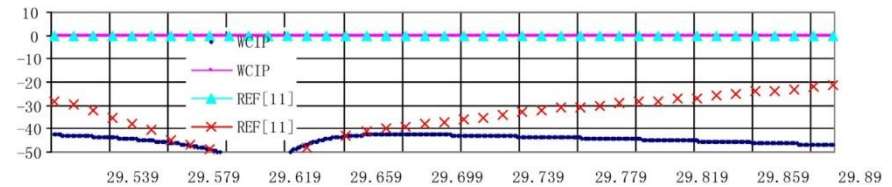


Figure 8. Variation of transmission and reflection coefficients as a function of frequency ($\theta = 16.4^\circ$).

5. Conclusion

The Wave concept Iterative Method and [11] have been described and utilised to investigate a complicated Frequency Selective Surface, and the comparison of the results throughout this research demonstrates a good agreement with those results. In Figures 6–8, a simple FSS structure as well as two sophisticated ones are investigated. The proposed method was validated by comparing our generated data to those from commercial software and recently released data.

References

- [1] Mitter, R., Chan, C.H. and Cwik, T. (1988) Technique for Analyzing Frequency Selective Surfaces—A Review. *Institute of Electrical and Electronics Engineers*, **76**, 1593-1615. <https://doi.org/10.1109/5.16352>
- [2] Munk, B.A. (2000) *Frequency Selective Surfaces: Theory and Design*. John Wiley & Sons, Inc., New York. <https://doi.org/10.1002/0471723770>
- [3] Kern, D.J., Werver, D.H., Monorchio, A., Lanuzza, L. and Wilhelm, M.J. (2005) The Design Synthesis of Multiband Artificial Magnetic Conductors Using High Impedance Frequency Selective Surfaces. *IEEE Transactions on Antennas and Propagation*. **53**, 8-17. <https://doi.org/10.1109/TAP.2004.840540>
- [4] Kim D.H. and Choi, J.I. (2006) Design of a Multiband Frequency Selective Surface. *Electronics and Telecommunications Research Institute Journal*, **28**, 506-508. <https://doi.org/10.4218/etrij.06.0205.0123>
- [5] Bliznyuk N. and Engheta, N. (2004) Numerical Study of Polarization-Dependant Focusing for a Bilayer Planar FSS Reflective lens at Millimeter Wavelengths. *Microwave and Optical Technology letters*, **40**, 361-365. <https://doi.org/10.1002/mop.11382>
- [6] Bhattacharyya, A.K. (1996) A Numerical Model for Multilayered Microstrip Phased-Array

Antennas. *IEEE Transactions on Antennas and Propagation*, **44**, 1386-1393.

<https://doi.org/10.1109/8.537333>

- [7] Bozzi, M., Perregrini, L., Weinzierl, J. and Winnewisser, C. (2001) Efficient Analysis of Quasi-Optical Filters by a Hybrid MoM/BI-RME Method. *IEEE Transactions on Antennas and Propagation*, **49**, 1054-1064. <https://doi.org/10.1109/8.933485>
- [8] Latrach, L., Sboui, N., Gharsallah, A., Gharbi A. and Baudrand, H. (2009) A Design and Modelling of Microwave Active Screen Using a Combination of the Rectangular and Periodic Waveguide Modes. *Journal of Electromagnetic Waves and Applications*, **23**, 1639-1648. <https://doi.org/10.1163/156939309789476428>
- [9] Sboui, N., Latrach, L., Gharsallah, A., Baudrand, H. and Gharbi, A. (2009) A 2D Design and Modeling of Micro Strip Structures on Inhomogeneous Substrate. *International Journal of RF and Microwave Computer-Aided Engineering*, **19**, 346-353. <https://doi.org/10.1002/mmce.20354>
- [10] Sboui, N., Gharsallah, A., Gharbi, A. and Baudrand, H. (2001) Global Modelling of Microwave Active Circuits by an Efficient Iterative Procedure. *IEEE Proceedings-Microwaves, Antenna and Propagation*, **148**, 209-212.

A. Sassi *et al.*

<https://doi.org/10.1049/ip-map:20010374>

- [11] Monorchio, A., Manara, G., Serra, U., Marola, G. and Pagana, E. (2005) Design of Waveguide Filters by Using Genetically Optimized Frequency Selective Surfaces. *IEEE Microwave and Wireless Components Letters*, **15**, 407-409. <https://doi.org/10.1109/LMWC.2005.850482>